Musical Acoustics

Third Homework

Report

Horn design

Students

Stefano Donà - 10868267
Paolo Ostan - 10868276

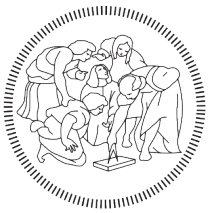

POLITECNICO
MILANO 1863

Introduction

Part 1): design of the exponential section

Introduction

In section *a)* and *b)* we evaluate the input impedance neglecting the impedance radiation at the mouth of the horn. We aim at comparing an approximation of the exponential horn with the analytical expression, and evaluate the degree of accuracy through the two metrics presented. In section *c)*, we're going to evaluate the accuracy of the approximation taking into account the radiation impedance at the mouth of the horn.

Analytical impedance

First, the analytical impedance of the exponential horn is computed. The geometry of the horn is visible in figure 1, while in figure 2 the computed horn shape is plotted.

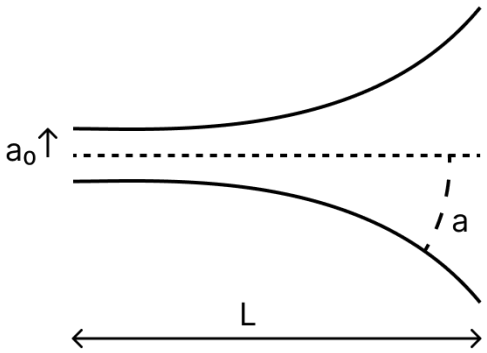

Figure 1: Horn Geometry

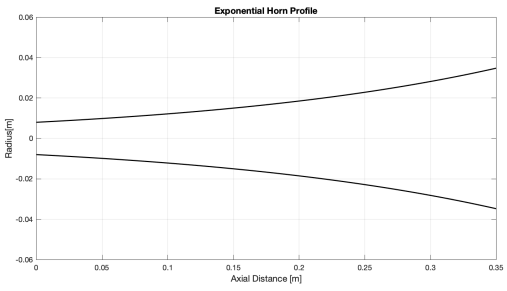

Figure 2: Horn Shape

Where the geometrical parameters are:

- $L = 0.35\ [m]$ is the length of the horn
- $a = a_0 e^{mx}\ [m]$ is the equivalent radius of the wavefront
- $a_0 = 0.008\ [m]$ is the equivalent radius at the throat of the horn
- $m = 4.2\ [m^{-1}]$ is the exponential growth factor of the horn flaring

Since the exponential horn belong to the family of Salmon horn, the wavefront can be considered planar and therefore the equivalent radius coincides with the effective radius of the circular (not spherical) surface at a specific coordinate. Moreover, we consider to have the system in standard environmental conditions so that the sound speed is $c = 343\ m/s$ and the air density is $\rho = 1.21\ kg/m^3$.
The analytical input impedance can be retrieved thanks to the formula:

$$Z_{in} = \frac{\rho c}{S_1}\left[\frac{Z_L cos(bL+\theta) + j(\rho c/S_2)sin(bL)}{jZ_L sin(bL) + (\rho c/S_2)cos(bL-\theta)}\right] \quad (1)$$

where $b = \sqrt{k^2 - m^2}$, $\theta = atan(m/b)$, $S_1 = \pi a_0^2$ is the throat surface, $S_2 = \pi(a_0 e^{mL})^2$is the mouth surface and $Z_L = 0$ since the flared opening ends towards air and the radiation impedence is neglected. The equation becomes:

$$Z_{in} = \frac{\rho c}{S_1}\left[\frac{j(\rho c/S_2)sin(bL)}{(\rho c/S_2)cos(bL-\theta)}\right] \quad (2)$$

and the frequency response in the interval $[0-2000]\ Hz$ is visible in figure 3

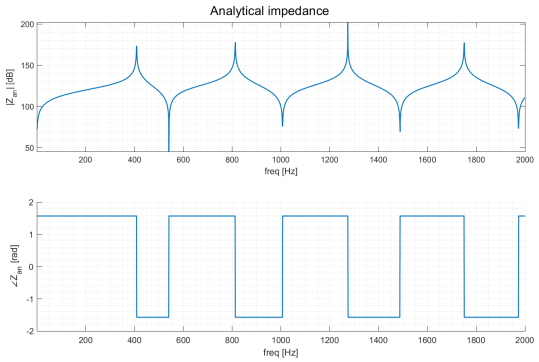

Figure 3: Analytical impedance

Approximated impedance

In this section we aim at approximating the exponential horn exploiting a concatenation of conical horns and verifying the validity of the model. In this particular step the radiation impedance at the mouth is neglected.In the following line the approximation strategy is thoroughly described. In order to evaluate the impedance of the whole horn the first segment considered is the last conical section. The input impedance of that is computed through the equation 3, recalling that the load impedance considered in this section is $Z_L = 0$. Once obtained it, the input impedance just evaluated is imposed as load impedance of the previous conical section, and the input impedance of the previous conical section is calculated. This is re-iterated through all the

sections that compose the horn until we reach the first conical section at the throat. A graphical example is visible in figure 4.

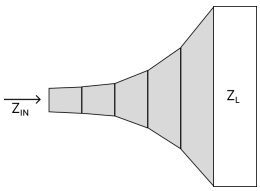

(a) Compound horn

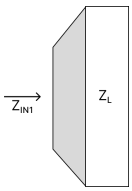

(b) First Step

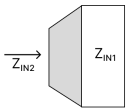

(c) Second Step

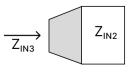

(d) Third Step

Figure 4: Steps to evaluate the input impedance of the approximated horn

$$Z_{in} = \frac{\rho c}{S_1}\left[\frac{jZ_L\frac{sin(kL-\theta_2)}{sin\theta_2} + (\frac{\rho c}{S_2})sin(kL)}{Z_L\frac{sin(kL+\theta_1-\theta_2)}{sin\theta_1 sin\theta_2} - (\frac{j\rho c}{S_2})\frac{sin(kL+\theta_1)}{sin\theta_1}}\right] \quad (3)$$

Where taking as reference the figure 5, S_1 is the surface at coordinate x_1, S_2 is the surface at coordinate x_2, and both coordinate are taken from the vertex of the considered cone. The parameter $L = x_2 - x_1$ is the length of the section and $\theta_1 = atan(kx_1)$ and $\theta_2 = atan(kx_2)$

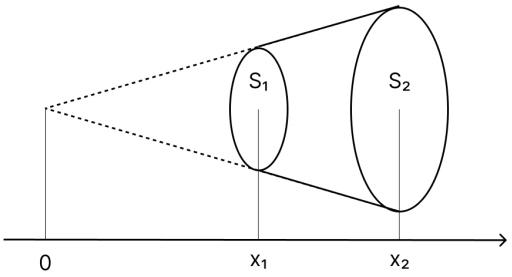

Figure 5: Cone section topology

Since the topology of the conical section is only specified by the trend of the radius of the horn we must retrieve the coordinates taking as reference the vertex of the cone. In order to do that we proceed obtaining the angular coefficient of the i-th conical section as:

$$\varphi = \frac{a(x_{i+\delta}) - a(x_i)}{x_{i+\delta} - x_i} = \frac{a(x_{i+\delta}) - a(x_i)}{\delta} \quad (4)$$

Thanks to the similar triangles properties we can consider:

$$\varphi = \frac{a(x_{i+\delta})}{x_2} = \frac{a(x_i)}{x_1} \quad (5)$$

finally the coordinates $x_{1,2}$ are retrieved as

$$\begin{cases} x_1 = \dfrac{a(x_i)}{\varphi} = \dfrac{\delta}{a(x_{i+\delta}) - a(x_i)}a(x_i) \\ x_2 = \dfrac{a(x_{i+\delta})}{\varphi} = \dfrac{\delta}{a(x_{i+\delta}) - a(x_i)}a(x_{i+\delta}) \end{cases} \quad (6)$$

Subdividing the length of the horn in N points, we obtain $N-1$ cones of length $\delta = L/N$. Once the number N is chosen, these steps have to be iterated $N-1$ times.
The module and phase curves of the impedance is shown below in figure 6 using 4 cones as the degree of approximation, the horn shape is plotted in figure 7.

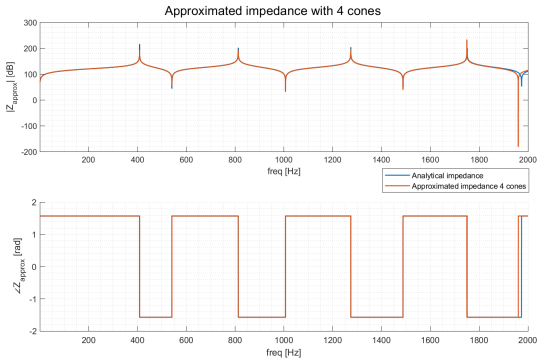

Figure 6: Analytical impedance vs 4 cones approximated impedance

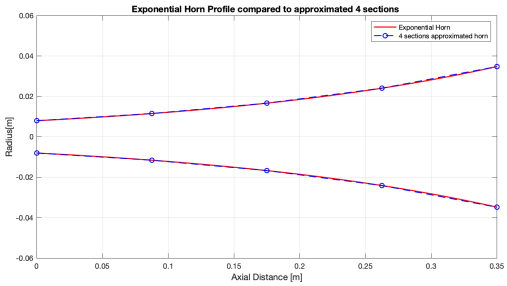

Figure 7: Exponential horn approximated to 4 conical sections

The evaluation of the errors brought in by the choice of the number of points is described in the following sections.

a) Error e_1 evaluation

In order to evaluate the difference between the analytical value of the impedance and the one approximated through the technique presented in the previous section the first metric of comparison used is the metric e_1, computed as:

$$e_1 = \frac{1}{(\omega_{max} - \omega_{min})}\int_{\omega_{min}}^{\omega_{max}} |Z_1(\omega) - Z_2(\omega)|^2 \, d\omega$$

Where Z_1 is the *analytical impedance* and Z_2 is *approximated impedance*, ω_{max} is the upper-bound of the

frequency range and ω_{min} is the lower bound of the frequency range. This metric allows to evaluate the mean square error between the two impedances. In figure 8 the *Mean Squared Error* is plotted as a function of the length δ of the conical sections.

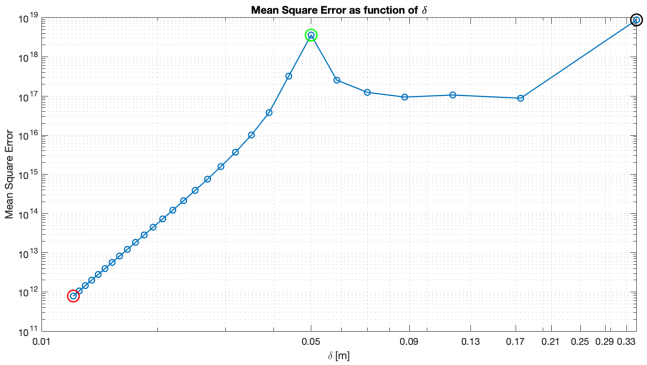

Figure 8: Mean Squared Error e_1

b) Error e_2 evaluation

The second evaluation method implemented is the evaluation of the difference in frequency between the maxima of the two impedances found in the frequency range considered $[f_{min}, f_{max}]$, we define the method e_2 as:

$$e_2 = \sum_{1}^{nRes} min|argMax_{\omega}abs(Z_1(\omega)) - argMax_{\omega}abs(Z_2(\omega))|$$

where $argMax_{\omega}abs(Z_1(\omega))$ is the way to find one of the resonance frequencies of the analytical impedance, while $argMax_{\omega}abs(Z_2(\omega))$ is the way to find one of the resonance frequencies of the approximated impedance. The values of the results in relation to the length of the conical section δ are plotted in figure 9, the term n_{res} is the number of resonances considered in the range of frequencies f_{min}, f_{max}.

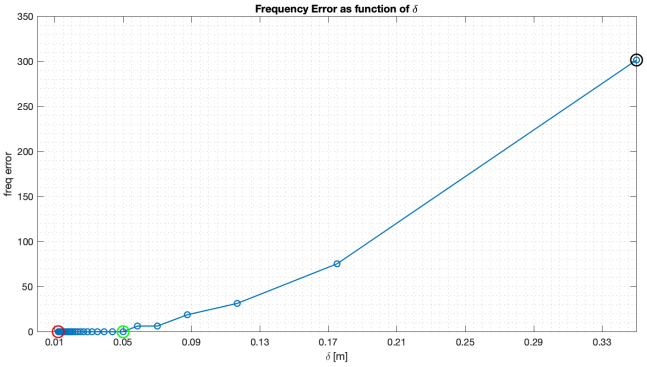

Figure 9: Difference in frequency between the maxima e_2 in the frequency range

The adoption of both metrics used as evaluation methods allows to improve the balance of the results obtained. For instance the first metric, taking into account the whole shape of the curves compared allows to have a precise index of the behaviour differences along the whole frequency-range. The combination with the second metric e_2 allows to balance the results focusing on the frequency position of the resonances. In figure 10 three cases of approximated impedances with different section lengths are plotted and compared to the reference analytical expression, while in figure 11 the approximated shapes are plotted in comparison to the analytical one. The case with shortest $\delta = 0.0121$ $[m]$ and the one with the maximum $\delta = 0.350$ $[m]$ is considered. The two horns are respectively composed of *29 conical sections* and *1 conical section*. An interesting example is the approximated horn with $\delta = 0.05[m]$, composed of 7 sections. It shows how the combination between the two metrics allows to evaluate more accurately the behaviour of the functions. The metric e_2 shows that the resonance frequencies are the same between the analytical impedance and the approximated-one, with an error value $e_2 = 0$. Differently, the metric e_1 presents a peak in this configuration with a value of $e_1 = 3.58 \cdot 10^{18}$. The results obtained are emphasized in figures 8 and 9 through the use of a red circle for $\delta = 0.0121$, a green circle for $\delta = 0.05$, and a black circle for $\delta = 0.350$.

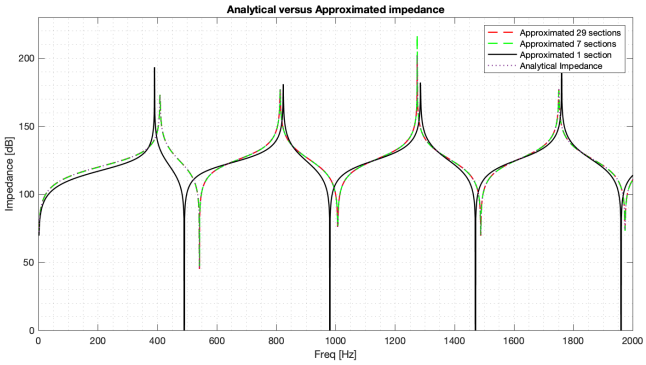

Figure 10: Analytical impedance compared to approximated with different section lengths

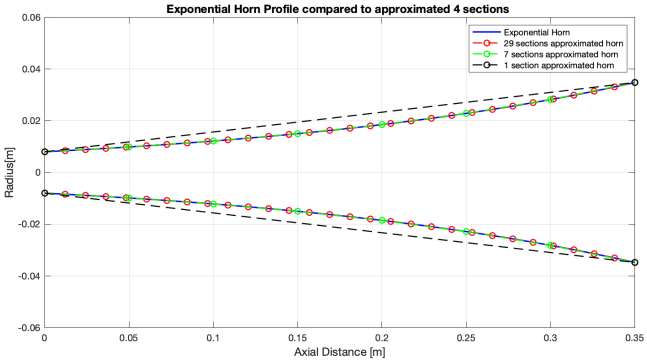

Figure 11: Exponential horn shape in three approximation cases

c) Impedance of approximated horn with radiation load

In the previous section the study of the approximated impedance has been computed and evaluated in relation to the analytical-one. Now the study is extended including to the model evaluated before the radiation load caused by the air external to the mouth of the horn. For the approximated horn the air can be modelled as an additional section with impedance:

$$Z_L(\omega) = Z_{L0}(\omega)\frac{S_p}{S_s}$$

the term Z_{L0} is defined as:

$$Z_{L0}(\omega) = 0.25\frac{\omega^2\rho}{\pi c} + 0.61j\frac{\rho\omega}{\pi a}$$

while S_p is the cross-sectional area of the cylinder and S_s the spherical wave front area at the open end of the cone, approximated as:

$$S_s = \frac{2S_p}{1+\cos\theta}$$

with θ the flaring angle of the last conical section, calculated as $\theta = atan(\frac{a_2}{x_{20}})$, where a_2 is the radius of the end of the mouth, while x_{20} is the distance of the mouth from the cone vertex used for the approximation.
In figure 12 the impedance of the approximated load is plotted. For the approximated horn the length of the conical section δ considered is $\delta = 0.05$, composed of 7 approximation sections, which is the value that produces the best precision for the metric e_2, with a value of $e_2 = 0$, employing the lowest number of conical sections to approximate the horn. It is also interesting to notice that this value produces a relative maximum for the metric e_1

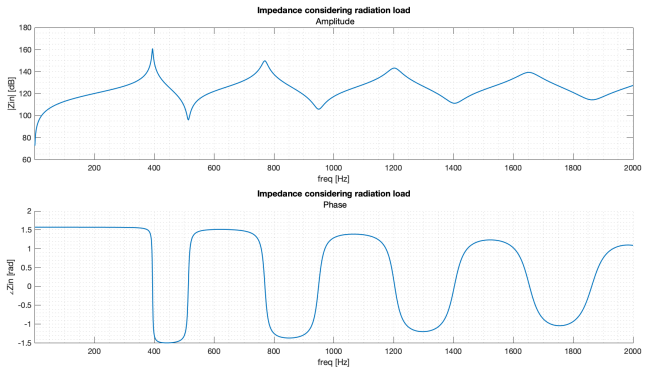

Figure 12: Approximated impedance considering radiation load

In figure 13 we can appreciate how the radiation load produces a shift of the peaks towards the lower frequencies and a smoothing in the magnitude and phase with respect to the input impedance of the unloaded horn. At high frequencies the peaks appear to be smoother and phase changes less steeper. This happens because, recalling the equation 3 since $Z_L \propto \omega^2$, the more we increase the frequency the more Z_L will dominate over the other terms. Computing now the error index e_1 between the *approximated impedance* considering the load and the one neglecting it. The result for the *Mean Squared Error* is therefore $e_1 = 2.587 \cdot 10^{18}$. A more relevant result is obtained computing the error between the approximated impedance with and without load with respect to the relative analytical impedances. In particular, in figure 14 the comparison between the approximated and analytical impedance considering the load is plotted, while in figure 15 the comparison is performed between the approximated and analytical impedance neglecting the presence of the load. Although the differences don't seem to be relevant by sight computing the error e_1 an important difference can be noticed. When considering the load the error between approximated and analytical impedance is $e_{1load} = 1.01 \cdot 10^{11}$ while not considering the load the error is: $e_{1noload} = 3.59 \cdot 10^{18}$. It can be noticed how, considering the load impedance the error along the whole frequency range decreases by 7 orders of magnitude. Moreover the result for the error obtained considering the load is lower than the best-one obtained not considering it, with $\delta = 0.0121$, which leads to $e_1 = 7.868 \cdot 10^{11}$.

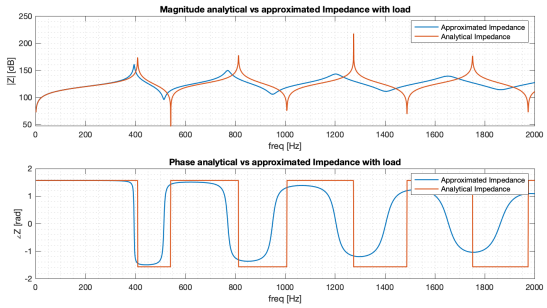

Figure 13: Approximated impedance with load vs without load

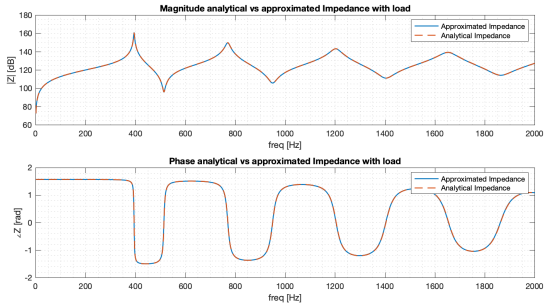

Figure 14: Approximated vs Analytical Impedance with load

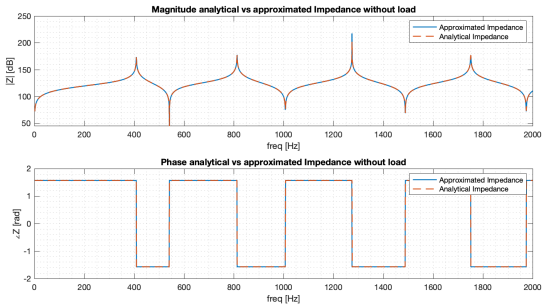

Figure 15: Approximated vs Analytical Impedance without load

Part 2: design of the compound horn

d) Impedance of compound horn

The goal of this section is to evaluate the impedance of the compound exponential horn smoothly joined with a cylindrical finite pipe of length $L_p = 0.85\ m$ and radius equal to the radius a_0, so that the system is similar to the one visible in figure 16. For the realization of the compound horn the exponential horn chosen is the approximated horn with 7 conical sections. In figure 17 the computed profile for the compound horn is plotted.

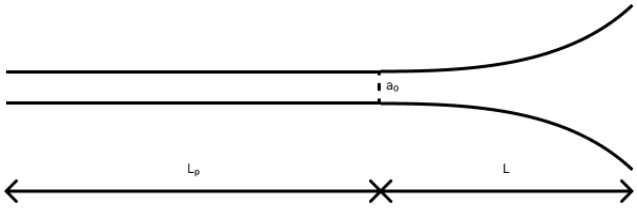

Figure 16: Structure of the compound horn

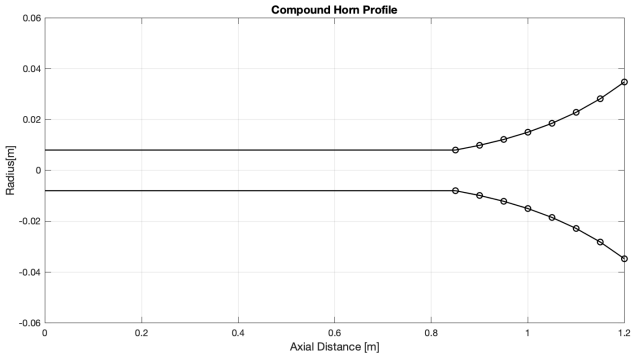

Figure 17: Compound horn plot

The relation that allows us to compute the impedance of a finite pipe is:

$$Z_{in} = Z_0 \left[\frac{Z_L cos(k_p L_p) + j Z_0 sin(k_p L_p)}{j Z_L sin(k_p L_p) + Z_0 cos(k_p L_p)} \right] \tag{7}$$

where $Z_0 = (\rho c)/S_p$ is the characteristic acoustic impedance of the air in the pipe, $S_p = \pi a_0^2$ is the pipe cross section, L_p is the length of the pipe and Z_L is the input impedance of the horn. Moreover, the wavenumber k_p is computed taken into account the wall losses of the pipe:

$$k_p = \frac{\omega}{\nu} - j\alpha \tag{8}$$

where:

$$\nu \approx c \left[\frac{1 - 1.65 \cdot 10^{-3}}{a_0 \sqrt{f}} \right] \tag{9}$$

$$\alpha \approx \frac{3 \cdot 10^{-5} \sqrt{f}}{a_0} \tag{10}$$

To verify the validity of these approximations, we introduce the term r_v, which indicates the ratio between the radius of the pipe and the boundary layer thickness, where the viscous losses acts on the particle velocity of the air. It can be computed as:

$$r_v = 632.8 a_0 \sqrt{f}(1 - 0.0029 \Delta T) \tag{11}$$

where $\Delta T = T - 300K$ considering $T = 293.15K$ as standard condition.
The approximations done in equations 9 and 10 are valid for $r_v > 10$ and usable down to $r_v = 3$, and we can use them since we're considering 1 Hz as minimum useful frequency of these analysis and therefore $r_{v,min} = 5.16$. The frequency behavior of the compound horn's impedance is plotted below in figure 18.

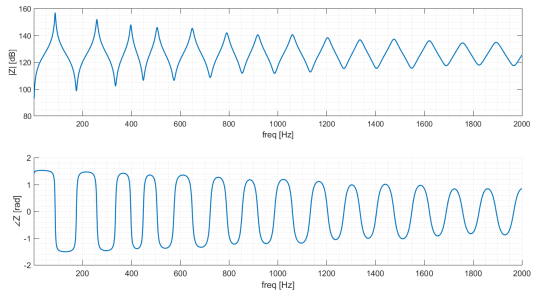

Figure 18: Impedance of the compound horn

We can clearly notice how the number of resonances is more than doubled, as in the interval $0 - 2\ kHz$ it reaches the number of 14 peaks, since the pipe introduces 10 resonances itself. The first ten maxima of the compound horn are reported in table 1.

id	freq [Hz]	id	freq [Hz]
1	87	6	790
2	258	7	917
3	397	8	1059
4	505	9	1203
5	649	10	1336

Table 1: First ten resonances of the compound horn

e) Inharmonicity evaluation

Now we're going to evaluate the harmonicity of the systems analyzed so far. We decided to report the value of harmonicity in *cents*, where 1 *cent* $= 1/1200$ *octave*. Therefore a semitone interval corresponds to an interval of 100 cents between two frequencies. In order to evaluate the difference in cents between two frequencies we exploit the inverse formula of the frequency relation:

$$f_n = \sqrt[1200]{2^n} \cdot f_{ref} \tag{12}$$

where f_{ref} is the reference frequency to take the interval from, and n is the number of cents. Taking the inverse formula, we can extract the parameter n as:

$$n = 1200 \; log_2 \left(\frac{f_n}{f_{ref}} \right) \tag{13}$$

Since we want to to evaluate the harmonicity with respect to the fundamental frequency ideal harmonicity $[f_0, 2f_0, 3f_0, \dots]$ we can rewrite the equation 13 as:

$$n = 1200 \; log_2 \left(\frac{f_n}{m f_0} \right) \tag{14}$$

where $m = 1, 2, \dots, M$ is the harmonic ID with respect to the fundamental frequency. The results of the computations are visible in figure 19.

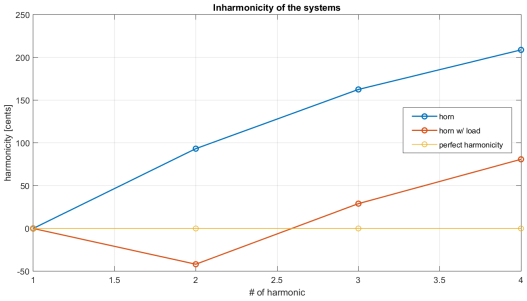

Figure 19: Inharmonicity of the horns

We can notice from this plot that the inharmonicity brought in by neglecting the load impedance at the mouth of the horn is higher than when it is taken into account. For the compound horn instead we evaluated the harmonicity with respect to the second resonant peak, doing so the equation 14 becomes:

$$n = 1200 \; log_2 \left(\frac{f_n}{m f_{ref}} m_{ref} \right) \tag{15}$$

where m_{ref} is the ID of the m-th harmonic with respect to the fundamental frequency and $m = 1, 2, \dots, M$. In figure 20 we can see what happens when we impose $m_{ref} = 1$ and $m_{ref} = 2$.
Using $m_{ref} = 1$ we can notice that the upper harmonics, or to be more precise, the resonances above the fundamental are highly inharmonic presenting and keeping a trend around 700 cents, which corresponds to approximatively a tonal interval of a fifth.

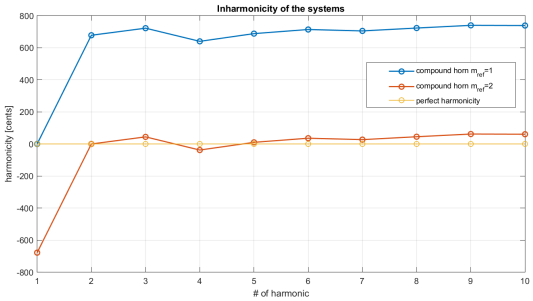

Figure 20: Inharmonicity of the compound horn

Taking, instead the harmonicity of the compound horn with $m_{ref} = 2$ we can appreciate that it is very bounded inside the interval $[-100, 100]$ *cents* except for the fundamental, that is highly inharmonic with respect to the other resonant peaks. This is closely related to the structure of the system, in particular to the inharmonicity brought by different impedance discontinuities, which are functions themselves of the shapes used [1].

References

[1] N. Fletcher and T. Rossing, *The Physics of Musical Instruments*, Springer New York, 2010.